AN IMPROVED METHOD FOR DETERMINING INFRASOUND BACK AZIMUTH WITH OPTICAL FIBER SENSORS

Kristoffer Walker, Mark Zumberge, Jonathan Berger, and Michael Hedlin

University of California, San Diego

Sponsored by US Army Space and Missile Defense Command

Contract No. W9113M-05-1-0020

ABSTRACT

Optical Fiber Infrasound Sensors (OFIS) are long compliant tubes wrapped with optical fiber that interferometrically measure the pressure variation along the length of the tube. Because each sensor averages spatially along the path of the tube, the response of the straight-line OFIS to the pressure variation is a function of the orientation of the OFIS relative to the back azimuth (BAZ) and incidence angle (INC) of the incoming wave. We have exploited this property with three 89-m-long OFIS having their azimuths separated by 120° and their centers separated by 77 m and have found that they can resolve the BAZ of most subhorizontal arrivals having good signal-to-noise ratio. We find a very good match between the BAZ determined from our technique and those determined from the same signals recorded on the co-located I57US microphone array using the Progressive Multichannel Cross-Correlation technique (RMS = 7°). We have also determined that a multi-arm OFIS can resolve the INC of the incoming signal.

OBJECTIVES

Optical Fiber Infrasound Sensors (OFIS) detect acoustic signals in the infrasound band (below 20 Hz), which propagate approximately in the horizontal plane. We defer a detailed instrument description to Zumberge et al. (2003). In general, a fiber is split into two fibers that are helically wrapped around a sealed, compliant tube in such a way that for an ambient pressure variation, the tube deforms and changes the optical path length difference *l* between the two fibers (Figure 1). The fibers are recombined and connected to a photodetector. The change in the path length difference is measured interferometrically by illuminating the photodetector with a 1310-nm laser. A lock-in amplifier is used to calculate the derivative of the fringe signal *y* while modulating the path length difference *l* by a small fraction of a wavelength at several hundred kHz with a piezoelectric crystal. When plotted against each other, the two fringe signals (*y* and *dy/dl*) trace out an ellipse. The angle swept out by the ellipse is empirically related to the pressure in real time at 200 Hz (Zumberge et al., 2004).

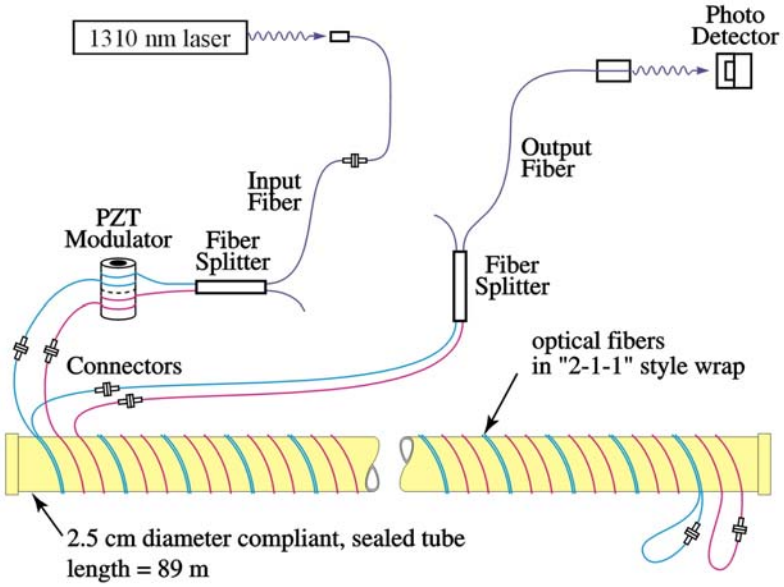

Figure 1. Schematic of one of four Optical Fiber Infrasound Sensor (OFIS) arms that are operating at PFO (I57US).

A multi-arm OFIS has several advantages over other infrasound sensors such as pipe and hose arrays. It is relatively inexpensive to build, deploy, and maintain. It is also easy to deploy, and requires much less space, making it highly portable (Figure 2). There is also evidence that in low-wind conditions, the noise floor of the OFIS is lower than the pipe and hose arrays for frequencies down to 1 Hz.

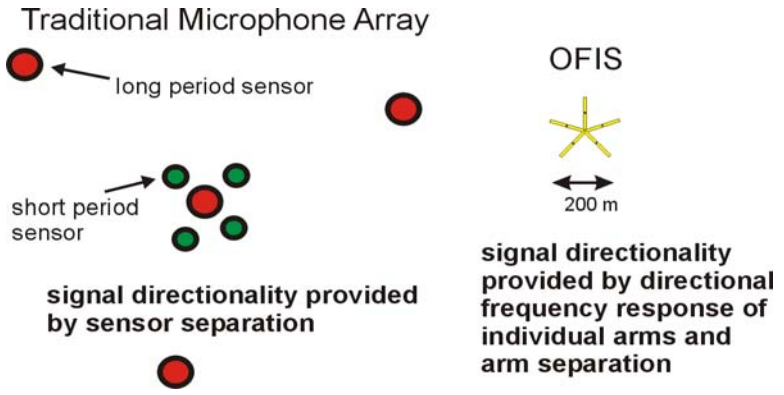

Figure 2. A typical International Monitoring System (IMS) infrasound array and a multi-arm OFIS shown to scale.

The objective of this research is determine if a ~200 m aperture multi-arm OFIS can be made to perform at least as well as a much larger (~1000-2000 m aperture) microphone array. In this paper, we (1) determine the number of OFIS and optimum configurations that are necessary to resolve the back azimuth of infrasound signals, (2) develop a generic technique for estimating back azimuths using an *n*-arm OFIS, (3) test the technique by comparing back azimuths estimated from synthetic signals and real signals recorded by a three-arm OFIS at Piñon Flat Observatory (PFO, I57US) in the southern California high desert, and (4) describe sensor uptime problems and solutions.

RESEARCH ACCOMPLISHED

Sensor Directivity

The response, *R*, of an OFIS relative to a point detector is a function of the orientation of the signal propagation with respect to the length of the OFIS:

$$R = \mathrm{sinc}\left(\frac{L\pi f}{V_a}\cos(\theta)\right) \quad (1)$$

where *f* is frequency, *L* is the length of the OFIS, V_a is the sound speed at the Earth's surface, and θ is the angle between the incident ray path and the OFIS.

$$\theta = \cos^{-1}(\cos(\theta_b)\sin(\theta_i)) \quad (2)$$

where θ_b is the back azimuth, and θ_i is the incidence angle. For typical telesonic infrasound signals, θ_i is approximately 90° (horizontal), and $\theta = \theta_b$. Figure 3a shows a polar plot of *R* as a function of angle from the long axis of the OFIS for three typical infrasound signal frequencies (assuming $\theta_b = 90°$).

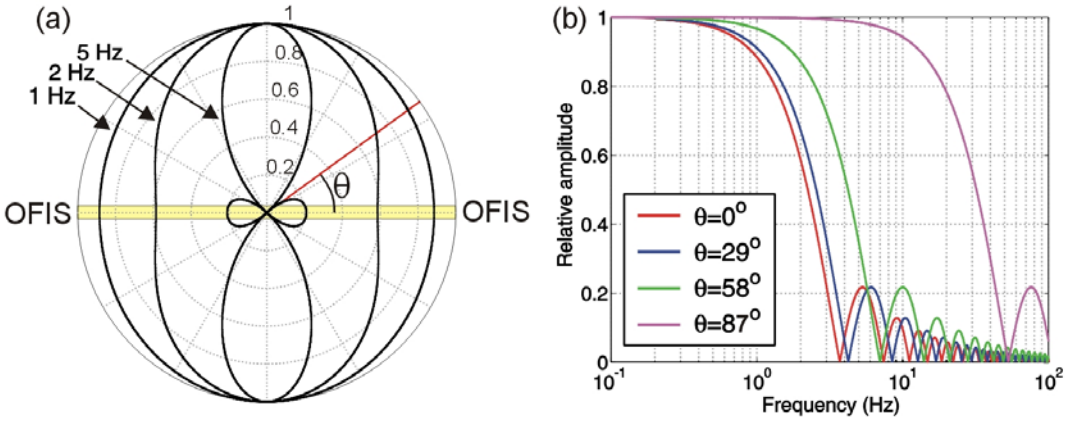

Figure 3. Frequency response *R* for an 89-m long OFIS at V_a = 340 m/s as a function of frequency and angle θ (eqns. 1-2).

The response *R* varies remarkably as a function of frequency, OFIS length, and acoustic velocity (Figure 3b). The phase of *R* is linear with respect to frequency, and corresponds to a static shift in the time domain. Therefore, if the back azimuth for a signal with a significant bandwidth is known, one can deconvolve *R* in frequency space from the recorded signal S_r to determine the actual signal waveform $S_w = S_r / R$.

Two-Arm OFIS

Because the response function is known for all signal orientations, one can record the signal of interest on two sensors with different orientations and "invert" for the signal by means of a grid search.

Algorithm

The recorded OFIS signal $S_r = f(S_w, \theta, V_a, L)$, where only S_w and θ are the unknowns. One can therefore estimate S_w and θ if one records the signal on two OFIS with different orientations (Figure 4)

$$S_{r1} = f(S_w, \theta) \qquad (3)$$

$$S_{r2} = f(S_w, \theta)$$

We do this by a substitution grid search, i.e., using S_{r1} to predict ${S_w}^p$, and then ${S_{r2}}^p$ for possible signal orientations

$${S_{r2}}^p = {S_w}^p R_2 = (S_{r1}/R_1)R_2. \qquad (4)$$

We can make the assumption (although not required) that the incidence angle θ_i = 90° and perform a grid search over only trial θ_b (between 0° and 90° from the OFIS 1 azimuth in 1° increments) to minimize the L2 misfit between S_{r2} and ${S_{r2}}^p$. However, the resolution power and accuracy is better when we minimize the sum of the L2 misfits between S_{r1} and ${S_{r1}}^p$ and S_{r2} and ${S_{r2}}^p$. The resolution is also much better if we perform a full grid search over trial θ_b and θ_i. We can perform the deconvolution in the frequency domain by using the water-level technique to avoid numerical instability; i.e., we raise all near-zero amplitudes in the denominator frequency spectrum to a "water level" of 1% of the maximum amplitude (e.g., Langston, 1979). We also can calculate formal 2σ error bars using the technique of Silver and Chan (1991), which assumes the misfit function is the sum of squares of a random chi-squared noise process.

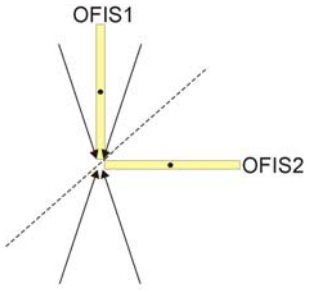

Figure 4. Layout of a two-arm OFIS in the 2-90 configuration. The dashed line is the plane along which arriving signals cannot be distinguished (azimuth of ambiguity). The arm centers are separated by 63 m to distinguish between the complementary set of 4 possible orientations from which arriving signals have identical shapes.

The configuration that offers the best signal orientation resolution for a two-arm OFIS is two arms separated by 90°, with their centers separated by at least 63 m. We call this the 2-90 configuration. Because an OFIS integrates the change in pressure along the length of the tube, one cannot determine the quadrant from which a signal originates (Figure 4). Any angle from OFIS 1 is part of a complementary set of four angles from which an incoming signal has identically recorded shapes on both OFIS. To get around this ambiguity for the 2-90 configuration, we exploit the fact that the two OFIS are separated by 63 m, and perform a cross-correlation during each trial θ_b to find the optimum time separation between S_{r2} and ${S_{r2}}^p$ before calculating the misfit. Then for the optimum θ_b, we check

the corresponding *dt*, which determines from which of the four angles it originated assuming θ_i = 45-90°. The resulting misfit function contains misfits from the optimally time-shifted S_{r2} and $S_{r2}{}^{p}$.

The angle halfway between both OFISs is an angle for which the recorded signals on both OFISs should be identical (Figure 4). We term this special angle the angle of ambiguity because one cannot resolve between it, its 180° complement, or a signal from directly above (θ_i = 0°).

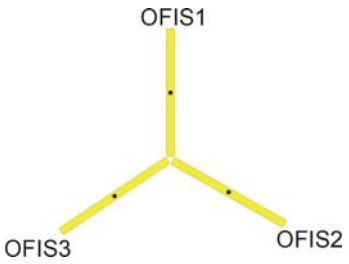

Figure 5. Layout of a three-arm OFIS in the 3-120 configuration. The arm center separations of 77 m eliminate any ambiguities in the arriving signal orientation.

Three-arm OFIS

The three-OFIS algorithm can easily be extended and applied to an *n*-arm OFIS. Our misfit function becomes the sum of the L2 misfits between the various predicted and observed OFIS recorded signals (sum of n^2 misfits). This requires much more CPU time. As a consequence, such an algorithm should be programmed in assembly language for real-time applications and optimized Fortran for research applications.

Testing the Algorithm on Synthetic and Real Data

The results of testing the algorithm for a two-arm OFIS in a 2-90 configuration were presented by Walker et al. (2004). They found that using the technique above, synthetic and recorded infrasound signals at PFO (spring 2004; I57US) when compared with those obtained by the co-located, 1.4-km wide microphone array (Hedlin et al., 2003) using the Progressive Multichannel Cross-Correlation algorithm (PMCC) (Cansi, 1995) suggest that a 2-90 OFIS is generally capable of resolving the back azimuth of signals that have a good signal-to-noise ratio, although there were a significant number of inaccurate measurements. In this section we report the results of testing a two-arm OFIS with a 120° azimuth separation (2-120 configuration) and a three-arm OFIS with a 120° separation (3-120). We calculate the resolution kernels using synthetic signals as well as compare recorded OFIS signal orientations to those determined using the PMCC method. We perform the analysis by (1) assuming horizontally traveling signals and searching only over the trial back azimuth, and (2) searching over both trial back azimuth and incidence angle. Due to the major increase in CPU time required for the additional search over incidence angle for a three-arm OFIS, we were required to convert our original Matlab algorithm into Fortran, although we developed a generic Matlab user interface.

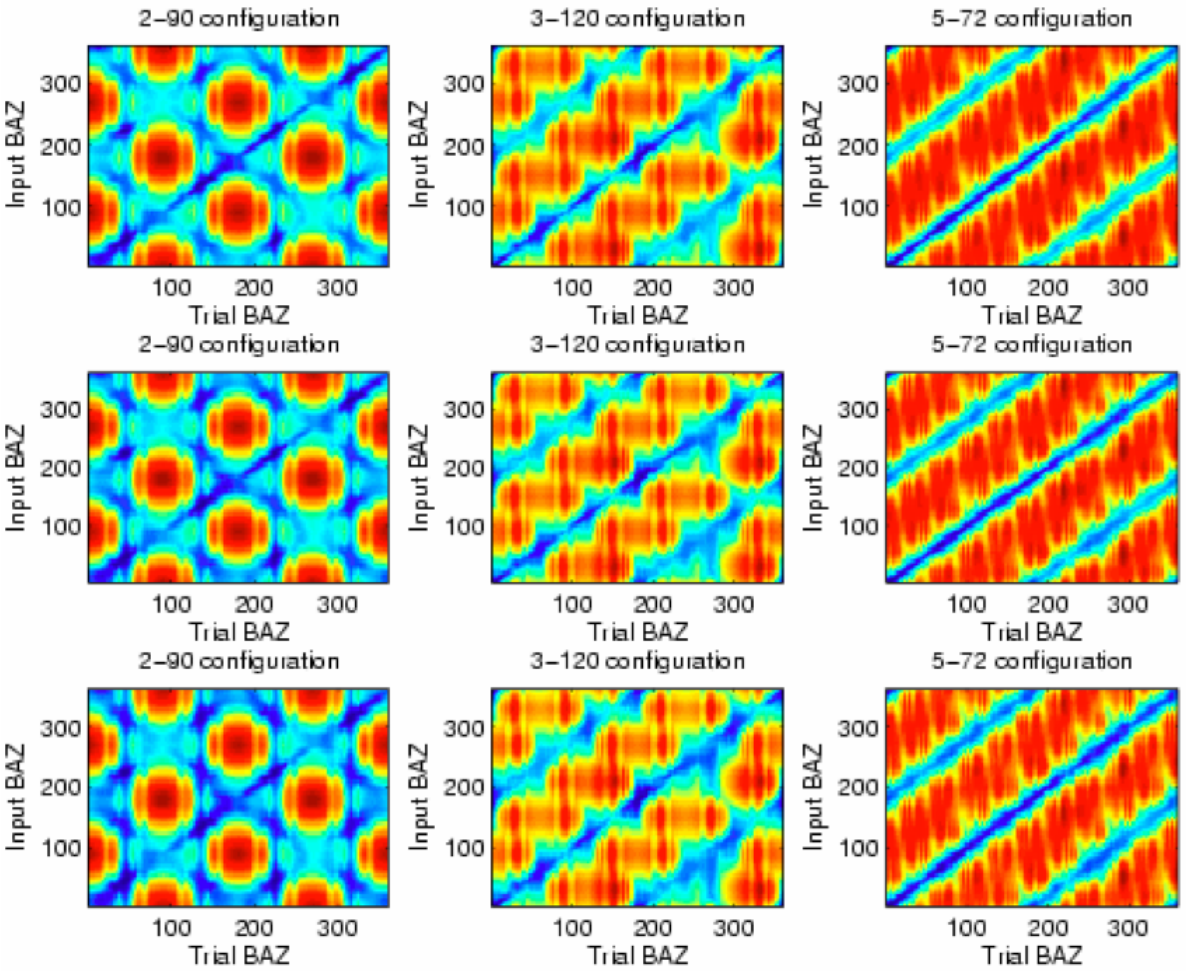

Figure 6. Resolution kernels of various OFIS configurations as a function of the trial back azimuth and the input back azimuth. These kernels were calculated using one of several possible algorithms, some of which are better than others.

Figure 6 compares the resolution kernels for the 2-90, 3-120, and 5-72 configurations (columns) at various input noise levels (rows). We created each 2D plot by generating synthetic waveforms for each input back azimuth assuming horizontally propagating signals. For each of these waveforms, the algorithm calculated the misfit function between the predicted and "observed" OFIS waveforms as a function of the trial back azimuth. Color indicates the log of the misfit: blues are lows and indicate the algorithm-determined back azimuth. In the ideal case, one expects to see a single blue line intersecting the origin with a slope of unity.

The most apparent feature for the 2-90 configuration plots are the complementary set of 4 orientations that yield similar misfit lows for most input back azimuths. For the input back azimuth of 45° (azimuth of ambiguity), one cannot determine between that orientation and its 180° complement.

2-120 configuration 3-120 configuration

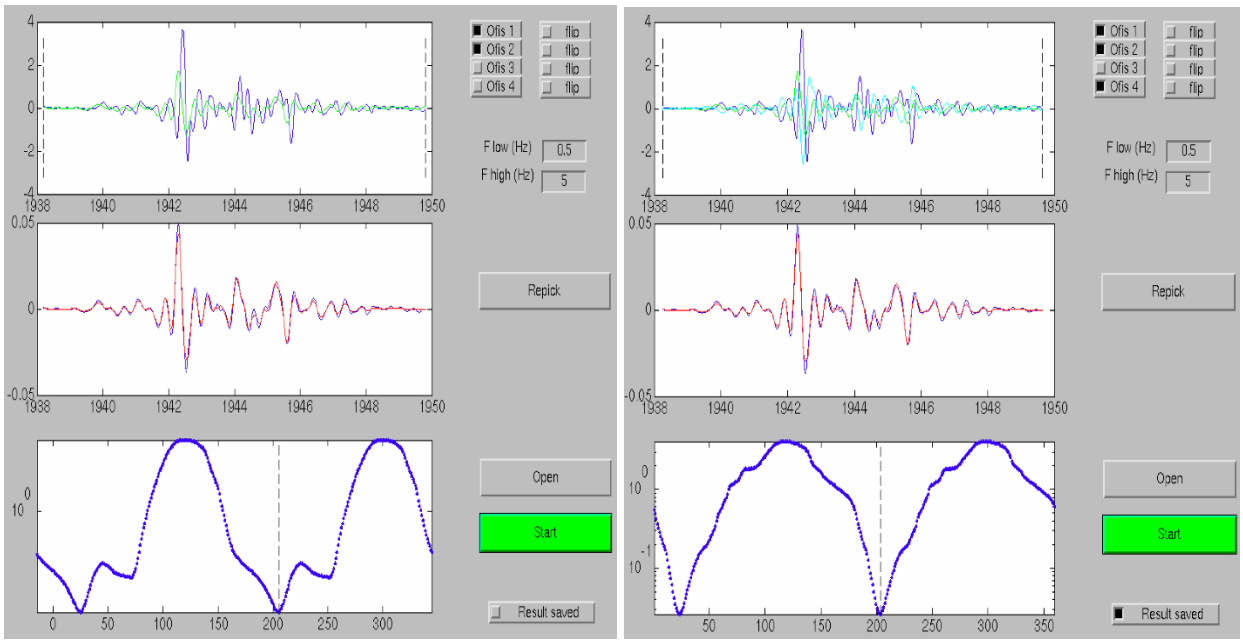

Figure 7. Characteristic plots for analyzing a signal recorded at PFO with a PMCC-determined back azimuth of 204° for a 2-120 (left) and 3-120 (right) configuration. The top plot shows the recorded OFIS signals as a function of time. The middle plot shows the optimum predicted and observed OFIS 1. The lower plot shows the log plot of the misfit as a function of the trial back azimuth. The vertical dashed line indicates the optimum OFIS-determined back azimuth. The misfits are identical in these plots because an unusual timing problem restricted our use of relative timing information, although we were still able to determine the correct hemisphere from which the signal arrived.

The situation is much better for the 3-120 configuration, as the correct resolution region (central blue line) is more consistent in size and shape. Although the azimuth of ambiguity problem is resolved, you can see to either side of the central blue line is a lighter blue line. Although present in the 2-90 results as well, these lines become distinctly visible now and represent the 180° complement of the set of 4 complementary orientations described above. Distinguishing between the true and 180° complement orientation for all configurations is strictly a function of the OFIS center separation. Therefore, the farther apart the centers, the warmer the colors of those lines.

The 5-72 configuration is nearly ideal in that the resolution region is quite consistent in size and shape. A 6-60 configuration would yield a nearly identical result. As with the 3-120 configuration, the 180° complement lines are clearly visible, although they are not mistaken for the true solution (colors are the log of misfit).

For all configurations, the noise level does not greatly affect the resolution kernel. This is intuitive because we are adding white noise to the synthetic waveforms before applying our preprocessing band pass filter and subsequent OFIS transfer functions *R*. Therefore, the spectral differences are not being greatly affected. The kernels would likely change considerably as a function of noise level if the noise was due to an acoustic source or if wind noise is spatially coherent over tens to hundreds of meters distance, which previous field experiments suggests is not.

During spring 2005, we recorded 24 signals of unknown origin at Piñon Flat Observatory on a 2-120 and 3-120 multi-arm OFIS configuration. Figure 7 shows the misfit functions for one of these signals for each configuration. Although both configurations resolve the correct back azimuth of 204°, the misfit function is more precise for the 3-120 configuration.

(a) (b)

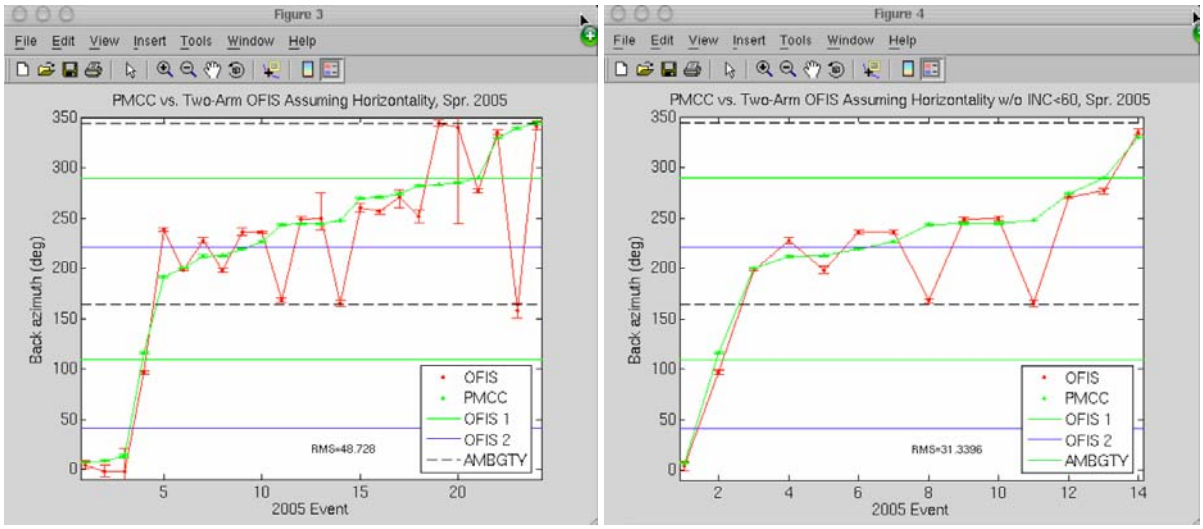

Figure 8. Comparison of the 2-120 OFIS and the I57US (PMCC) back azimuths determined for signals recorded during spring 2005. Events are sorted by PMCC back azimuth. (a) Results for all 24 signals. (b) Subset of signals for which the OFIS-determined incidence angle was 60-90°. PMCC was only permitted to search between θ_i = 60-90°.

We determined the true signal orientation by the co-located, 1.4-km aperture I57US microphone array using the PMCC method. Only 5 elements were operating during this time, so the accuracy of the reference signals is not well known. We also only allowed PMCC to search for signals with incidence angles θ_i = 60-90°. When we compare the back azimuths determined by PMCC and the 2-120 configuration assuming horizontally traveling signals, we see that there is considerable scatter with an RMS error of 49° (Figure 8a). However, when we use our algorithm with the 3-120 configuration, we identified many signals for which the θ_i<60°. Figure 8b shows the subset of 2-120 and PMCC back azimuths for θ_i>60°. This more valid comparison yields an RMS error of 31°. Better results were generally obtained with the 2-90 configuration (Walker et al., 2004).

A 3-120 configuration yields much better results (Figure 9a). By simply assuming horizontally traveling signals, the RMS error was reduced by half to 16°. By only considering those signals with θ_i = 60-90°, the RMS error is further reduced to 9° (Figure 9b). The RMS error decreases to 7° when we use the back azimuths determined during the full search over trial θ_b and θ_i (Figure 9c).

The results in Figure 9 suggest that incidence angle is a very important quantity that should not be ignored if back azimuth accuracy is desired. These results also raise the question of how well incidence angle is resolved. Figure 10 shows a color plot of the misfit as a function of back azimuth and the incidence angle for a nearly horizontally traveling signal and one with a moderate incidence angle. A single orientation is not well resolved in (b), which may be due to a fast moving source (e.g., meteor), a signal with a narrow bandwidth, or a poor resolution of incidence angle for that particular signal orientation. A resolution kernel as a function of the incidence angle and configuration must be further investigated. The distinct separation between orientations in (b) may be due to the PMCC limit of θ_i = 60-90°.

(a) (b)

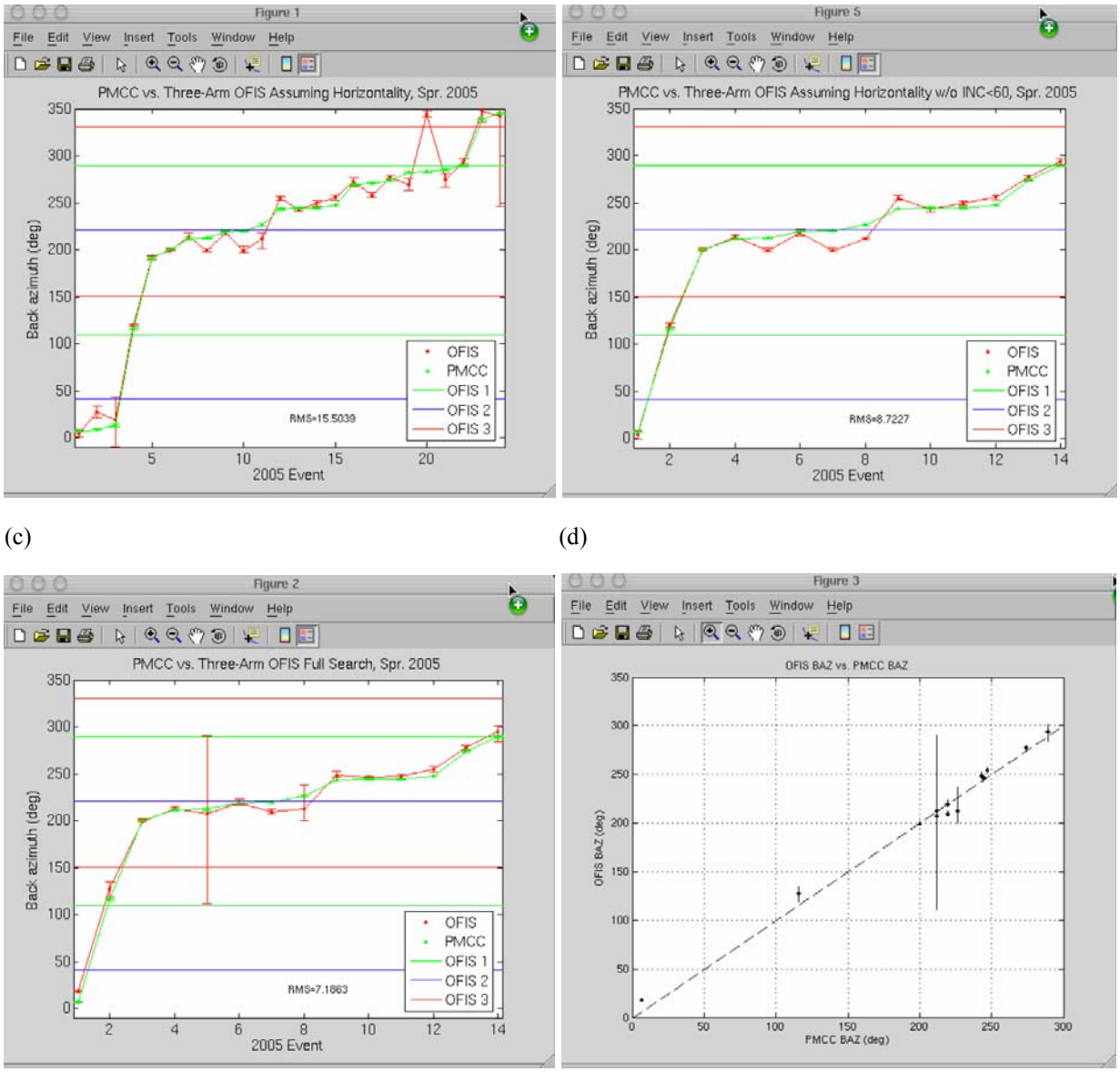

(c) (d)

Figure 9. Comparison of 3-120 OFIS and I57US (PMCC) back azimuths. Shown are (a) all results assuming horizontally traveling signals, (b) subset of (a) for signals with θ_i = 60-90°, (c) same events as in (b) but using back azimuths determined during full search over θ_b and θ_i, and (d) plot of OFIS back azimuth in (c) versus PMCC back azimuth.

The results in Figure 9 suggest that a three-arm OFIS in a 3-120 configuration can determine the back azimuth and incidence angle of an incoming signal. The close similarity to back azimuths determined via the PMCC method, the results in Figure 10, and the limited number of I57US elements used raises the question of the accuracy of our PMCC results. Walker et al. (2004) found that the orientation of each OFIS to within 0.3°. They also performed an analysis on the I57US orientation by using PMCC to analyze the signals of 16 known regional mine-blast events from θ_b = 280-340°, and found that the theoretical θ_b matched those from PMCC within 10°. It is therefore possible that the OFIS back azimuths and incidence angles are more accurate than those provided by PMCC.

(a) (b)

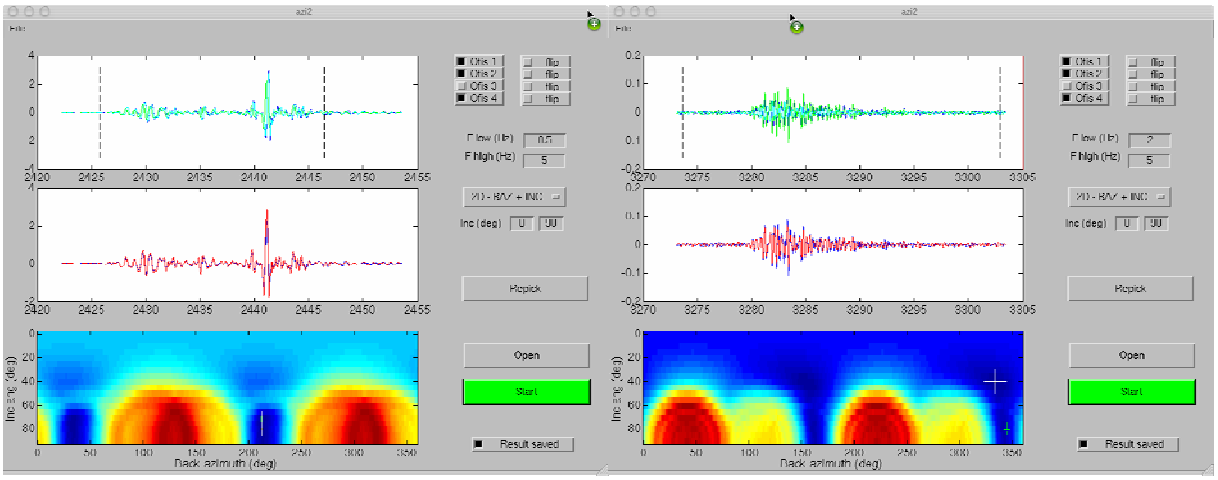

Figure 10. Resolution of incidence angle and source motion for signals of unknown origin for a 3-120 configuration. Shown are results of a full search over trial θ_b and θ_i for a nearly horizontally traveling signal (a) and one with a moderate incidence angle (b). Axes are as in Figure 7, except the lower plot shows the log of the misfit (blues are lows) as a function of trial θ_b and θ_i. The white and green pulses indicate the OFIS- and PMCC-determined signal orientations, respectively.

Figure 9d shows that most of our results were for signals from the western hemisphere. Ideally one needs to repeat such a study at a field site with a larger variety of known source locations.

Problems and Solutions that Affect OFIS Uptime

There are two problems that we have identified that affect OFIS uptime. The first and most problematic is that due to differential polarization change of the split laser beam in the two fibers wrapped around the OFIS. The fringe signal *y*, which is necessary to recovering the pressure change, is created by the interference between the recombined laser beams from each of the two fibers wrapped around the OFIS. This interference is associated with the change in the differential optical-fiber path length. In order to obtain *y* the laser in the two fibers must have the same polarization when they are recombined just before the photodetector. If one of the fibers has a polarization that is orthogonal to the other, no interference will occur and the fringe signal will not develop. We have confirmed that the difference in the polarization between the two fibers changes greatly as a function of OFIS temperature. This is especially a problem during the hot summer months.

Our OFIS prototype tube is black. Consequently, it heats up greatly in the sun. When clouds pass overhead, it cools off. At times the polarizations would become mutually orthogonal, sometimes several times per hour. We found that covering the tube with a white polyvinyl chloride (PVC) outer covering eliminates a great deal of OFIS temperature fluctuation and subsequent differential polarization change. However, ambient air temperatures still greatly affect this. We experimented with an alternative solution using a polarization scrambler. This instrument rapidly changed the input polarization and we applied a low-pass filter on the photodetector output. Unfortunately the polarization was changing too greatly for this technique to work.

We also experimented with a diversity detector. In this solution, one uses a series of polarizing beam splitters to recombine the two fibers along three different polarization angles. Each recombined beam goes to a photodetector. We confirmed that this technique with two recombined beams/photodetectors works by visually monitoring the two ellipses in the field during the course of a day. When one ellipse began to collapse, the other ellipse got bigger. This is currently our preferred method for dealing with polarization change, and we are in the process of evaluating a variation of this solution that will enable us to work with only one composite ellipse (rather than two or three).

The other problem we encountered is spiking in the pressure data. The problem is the worst beginning at sunset when the outside temperature begins to fall rapidly, but continues well into the early morning of the following day.

We have identified the source to be creaking between the fiber and OFIS silicone tube. This creaking has been demonstrated in the laboratory, and occurs when the grip of the fiber around the tube is loosening. Such a situation occurs most evenings at sunset when the falling temperature cools the tube causing it to shrink. This problem is far worse on OFIS arms that we have moved in the field from their originally deployed position. We twisted a problem OFIS arms to tighten the grip between the fiber and the silicone. This greatly reduced the spiking problem, although itchanged the calibration factor (and possibly calibration consistency along the OFIS). We believe a pressurized OFIS silicone tube at ~1 psi above the ambient will be enough to eliminate the spiking problem and preserve the consistency in calibration.

CONCLUSIONS AND RECOMMENDATIONS

We confirm that three OFIS arms with angular separations of 120° and centers separated by 77 m are fully capable of resolving the back azimuth of telesonic infrasound signals that have a good signal-to-noise ratio with the algorithm we present above. Tentative results also suggest that a 3-120 configuration can also resolve the orientation of signals with moderate incidence angles, although this needs to be confirmed by additional analyses. For two OFIS arms, an angular separation of 90° provides better back azimuth (and probably incidence angle) resolution and a faster algorithm speed than for an angular separation of 120°. We suggest that a five-arm OFIS with arms laying on the ground, azimuth separations of 72°, and an aperture of 200 m provides the best resolution in back azimuth and incidence angle for infrasound signals with a central frequency of 2-5 Hz.

Our results are highly significant because they indicate that a multi-arm OFIS, acting as a directional antenna, is capable of providing the same directional information as an array of conventional rosette filters while covering much less space. Conventional arrays rely on time delays between elements to determine θ_b and θ_i, requiring significant separation between elements (several hundreds to thousands of meters) to produce time differences. The OFIS reliance on directional frequency response (and to a less extent time delays) provides the same information within a more localized area (Figure 2)—a significant advantage when space is at a premium (e.g., on island sites) and maintenance costs are high.

ACKNOWLEDGEMENTS

We are indebted to Matt Dzieciuch, Petar Durdevic, and Pat Walsh and for their time and effort in software/hardware development and field work. We thank the US Army Space and Missile Defense Command for sponsoring this project (Contract No. W9113M-05-1-0020).

REFERENCES

Cansi, Y. (1995), An automatic seismic event processing for detection and location: the P.M.C.C. method, *Geophys. Res. Lett*. 22: 1021.

Hedlin, M.A.H., B. Alcoverro, and G. D'Spain (2003), Evaluation of rosette infrasonic noise-reducing spatial filters, *J. Acoustic. Soc. Am.* 114: 1807.

Langston, C.A. (1979), Structure under Mount Rainer, Washington, inferred from teleseismic body waves, *J. Geophys. Res.* 84: 4749.

Silver, P.G., and W.W. Chan (1991), Shear-wave splitting and subcontinental mantle deformation, *J. Geophys. Res.* 96: 16, 429.

Walker, K.T., S. Arrowsmith, J. Berger, M. Hedlin, and M. Zumberge (2004), Resolving infrasound signal back azimuths with arrays of optical fiber sensors, in *Proceedings of the 26th Seismic Research Review*: *Trends in Nuclear Explosion Monitoring,* LA-UR-04-5801, Orlando, FL, 680-687.

Zumberge, M.A., J. Berger, M.A.H. Hedlin, E. Husmann, and S. Nooner (2003), An optical fiber infrasound sensor: A new lower limit on atmospheric pressure noise between 1 and 10 Hz, *J. Acoust. Soc. Am.* 113: 2474.

Zumberge, M.A., J. Berger, M.A. Dzieciuch, and R.L. Parker, (2004), Resolving quadrature fringes in real time, *Applied Optics* 43: 771-775.